JOURNAL OF MATERIALS SCIENCE 33 (1998) 859–867

A broad-line nuclear magnetic resonance study of water absorption and transport in fibrous cement roofing tiles

A. J. BOHRIS, B. NEWLING, P. J. McDONALD
Department of Physics, University of Surrey, Guildford, Surrey GU2 5XH, UK
A. RAOOF, N. L. TRAN
Laboratoire Central des Ponts et Chaussees, Cite Descartes, 2 Allee Kepler, 77420 Champs sur Marne, France

The ^{1}H nuclear magnetic resonance spin–spin relaxation time of water in a fibrous cement roofing tile has been measured as a function of hydration using the Carr–Purcell–Meiboom–Gill pulse sequence with a pulse gap sufficiently short to negate most of the attenuation effects of water diffusion in the pore space magnetic susceptibility gradients of the tile. The data reveal pores with three characteristic sizes, consistent with earlier mercury intrusion porosimetry results and details of the manufacturing process. The relaxation times are constant as a function of hydration, suggesting that, at intermediate hydrations, some pores fill completely while others remain empty. There is also evidence that the smallest pores fill first. Complementary imaging studies reveal a three-layered heterogeneous structure which is consistent with the manufacturing process. The images show the establishment of a dynamic equilibrium water concentration gradient across the slate when one side is exposed to water. The mutual diffusion coefficient of water in the tile is estimated as 4×10^{-7} cm^2 s^{-1}. Finally the effects of a water-resistant coating on water transport are shown. © *1998 Chapman & Hall*

1. Introduction

The understanding and control of water transport in porous ceramic building materials are crucial to the durability of large-scale civil engineering structures. One component of many of these structures is fibrous cement roofing tiles. A high-quality tile must clearly be resistant to rapid water transport but must also, over longer periods of time, allow some breathing of water vapour. Moreover, it is important that the tile retain its shape over time and that it does not bend when exposed to a humidity gradient across its two surfaces. Current methods of assessment of water transport in roofing tiles are largely inadequate. For instance gravimetric or mass uptake methods do not give any information about the spatial distribution of the water. On the other hand, methods which are spatially resolved, such as electron microscopy, are generally destructive, so prohibiting time course studies. Other techniques such as infrared or colour analysis give only surface information.

A powerful method for obtaining both spatially and non-spatially resolved information about water concentration and mobility in materials systems is nuclear magnetic resonance (NMR) [1–3]. Measurements of the ^{1}H NMR relaxation times can be used to infer pore size information [4]. These techniques are increasingly used for the study of cementitious systems [5, 6]. In this paper we report ^{1}H relaxation time measurements as a function of water content for an industrial fibrous cement roofing tile, equilibrated in a range of relative humidities and under water-saturated conditions. Additionally we report spatially resolved measurements of the development of the water concentration profile across the tile for a series of dry tiles exposed to water. Broad-line magnetic resonance imaging techniques, specifically stray field imaging [7, 8], have been used for this purpose because it is well known that magnetic susceptibility field gradients, paramagnetic impurities and binding of water molecules to pore surfaces all increase the natural linewidth of the water in the cement and hence prohibit the use of more conventional Fourier techniques. Stray field imaging overcomes these difficulties and therefore yields quantitative information.

2. Experimental procedure

Two types of artificial fibrous cement tile manufactured by Everite SA, France, have been studied. These tiles have already been the subject of a detailed study by conventional methodologies [9], the important results of which are summarized here. The tiles used are those labelled series A-UP and B-UP in [9]. The series A-UP tiles are composed of 78% ordinary

Portland cement, 10% asbestos fibres, 10% filler and 2% colourant. The water-to-cement ratio used in manufacture is 0.25. They are prepared by pressing the raw material through rollers in three stages followed by appropriate curing. This processing results in the series A-UP tiles characteristically exhibiting a three-layered structure, with, we suggest, the layers differentiated by average pore size. The outer (upper) surface of the tile in a roofing application is generally smoother than the inner surface and is formed by the layer with the smallest average pore size. The overall thickness of the tiles is 3.6 mm. The series B-UP tiles are identical with the series A-UP tiles except that a further layer is added during manufacture which increases the thickness to 4.1 mm. This layer composed primarily of cement and sand is designed to reduce bulk water ingress into the slate. All the bulk analysis described in this paper has been performed on series A-UP tiles. The imaging work has been carried out on both series A-UP and series B-UP tiles in each case with either the inner or the outer tile surface exposed to water.

Fig. 1 shows the pore size distribution for the series A-UP tiles as measured by mercury intrusion porosimetry. The pore size distribution shows a trimodal tendency with characteristic pore sizes of 0.015, 0.15 and 1.5 μm. According to the mercury intrusion result, there is approximately equal volume in each pore size. The overall porosity by mercury intrusion is 16.8%. Fig. 2 shows the mass uptake of water as a function of relative humidity for these tiles on the left-hand axis, together with the relative saturation on the right-hand axis. Full hydration obtained by vacuum saturation of an oven dried tile is 17.2%. This last result is the average of those reported in [9] and new measurements carried out on the batch of tiles used in this study. The overall porosity measured by water suction is 35% according to [9], substantially more than measured by mercury porosimetry. The discrepancy between mercury and water porosity measurements has been discussed more fully by Raoof and Sabouraud [9] and has been reported more widely for other systems [10]. The discussion focuses on the fact that the mercury fails to intrude the smallest pores, so that we might expect relatively greater volume in the small pores than suggested by Fig. 1. Moreover, the mercury can damage the pore structure.

For the bulk analysis, a range of samples was equilibrated at different relative humidities in the range 4–97% over saturated salt solutions. Equilibration generally took of the order of 4 weeks. The samples were then sealed in glass tubes with a solid glass rod taking up the majority of the free volume. Additionally, an oven-dried and vacuum-saturated tile sample was prepared. Measurements of the ^{1}H spin–spin relaxation time were made at room temperature using pulse-free induction decay and Carr–Purcell–Meiboom–Gill (CPMG) multiple-spin-echo experiments [11]. In both experiments, the NMR field strength was 0.5 T and the pulse length was 3 μs. In the case of the free induction decay, the spectrometer dead time and bandwidth were 8 μs and 1 MHz, respectively, consistent with observing short T_2 components in the signal. In the case of the CPMG experiments the pulse gap was varied widely between 12 and 200 μs. The reason for the use of such a large range of pulse gaps, and in particular small pulse gaps, was the requirement to minimize the effects of water diffusion in the susceptibility gradients of the pore space, which reduces the observed T_2 relaxation time.

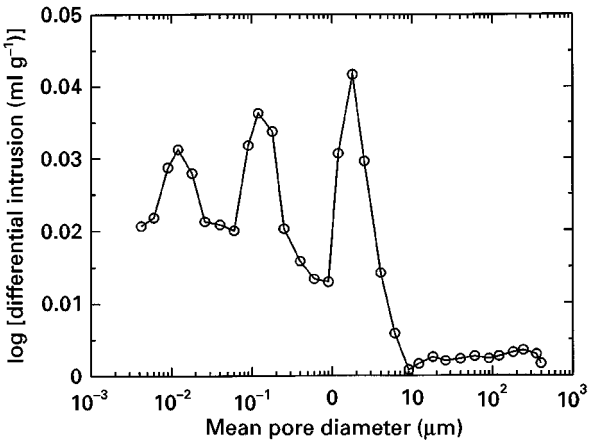

Figure 1 The pore size distribution of a series A-UP tile measured by mercury intrusion porosimetry.

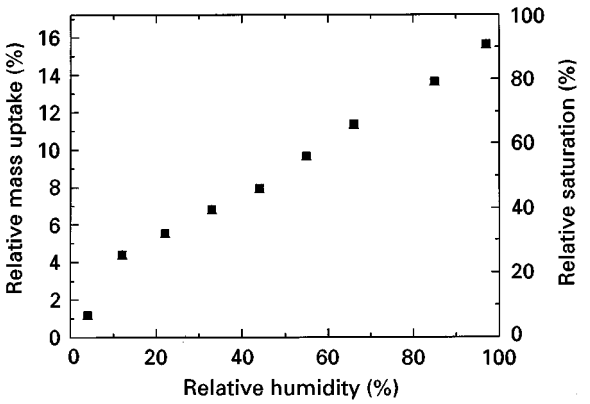

Figure 2 The fractional mass uptake of water (left-hand axis) by a series A-UP tile as a function of relative humidity. The right-hand axis shows the hydration level relative to a mass uptake of 17.2% at full saturation.

For the magnetic resonance imaging studies, pieces of material in disc form 8 mm in diameter were cut from the tiles and mounted in glass tubing using a small quantity of epoxy resin. Samples with both the outer and the inner surface uppermost were prepared. The prepared samples were oven dried at 110 °C for several days until the sample mass was stable. The dry tiles were then profiled in the stray field apparatus. The magnetic field strength was 5.5 T and the gradient strength 58 T m^{-1}. The measurements were made using a standard multiple-quadrature-echo sequence [7, 8] with a pulse gap of 14 μs, a pulse length of 6 μs and a step size (resolution) of 200 μm. Typically 64 averages were acquired over 20 min. Water was then added to the tube above the tile with the other surface left exposed to the laboratory atmosphere which had an average relative humidity of 30%. In a first experiment, these samples were imaged after 30 h and then periodically over 3 weeks. In a second experiment, the

samples were imaged at 40 min intervals during the 24 h immediately following the addition of water.

3. Results and discussion

3.1. Bulk analysis

Fig. 3a shows a representative free induction decay, and Fig. 3b representative CPMG echo train data for two different pulse gaps, τ, of 12 and 50 μs recorded from a tile equilibrated at 97% relative humidity. The free induction decay shows a large component with a very short decay constant. This signal is attributed to the hydrogen present both in the hydration products of the cement and in mobile water filling the capillary pores. The asbestos fibres are mineral in composition and devoid of hydrogen. The free induction decay can be fitted to an exponential with a time constant, T_2, of the order of 7 μs, although it is realized that other functions provide a more exact description of such rapid decays. Back extrapolating the data to zero time suggests a relative intensity of 0.43 that of a corresponding volume of bulk water. Consequently, this sample contains hydrogen equivalent to a total of 43% water by volume, broadly consistent with its manufacture and hydration state.

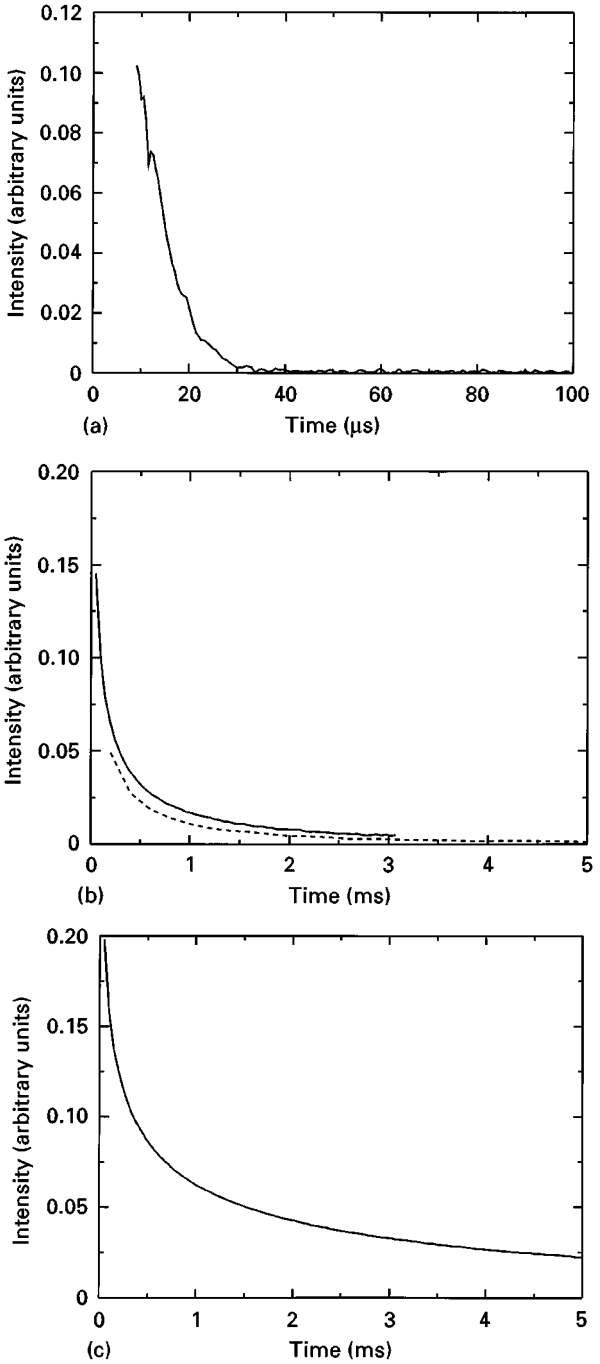

Figure 3 (a) The free induction decay signal recorded from the 97% RH tile. (b) The CPMG echo train decay signal from the same tile recorded with a pulse gap of 12 μs (——) and 50 μs (– – –). (c) The CPMG echo train decay signal from the vacuum saturated tile recorded with a pulse gap of 12 μs.

The signal due to mobile water in the pore structure can be separated from that due to hydration products because of their inherently different relaxation mechanisms: strong dipolar interaction in the case of the hydration products as against diffusion in the magnetic susceptibility gradients created by the pore structure in the case of the mobile water. Attenuation due to diffusion is eliminated in a CPMG experiment in the limit of a zero pulse gap whereas dipolar attenuation is not.

The analysis of the CPMG data is complicated by the fact that the water decay is of a multiple-exponential nature, each component representing water in a different pore environment. Attempts have been made to fit the data to single-, multiple- and stretched-exponential decay functions. In general, a single exponential is inadequate to fit the CPMG data. For low hydrations, a reasonable fit can be made using just two components. However, given the *a priori* knowledge that the tile consists of three layers and that it has three characteristic pore sizes, and in the light of the profiling studies reported below, three component fits have also been attempted. In the wettest tiles in particular, the three components are well resolved and yield a significantly improved quality of fit compared with just two components. It is the results of the three component fitting which are presented here. The fits have been carried out using the software package Easyplot. The pulse gap dependence of each of the three T_2 components is shown in Fig. 4a for the tile equilibrated at 97% relative humidity (hereafter called the 97% RH tile) together with, in Fig. 4b, the relative amplitudes of these components. We note that the mass uptake for this sample was 15.6%, corresponding to 31% hydrated porosity. As the pulse gap, τ, is increased, so the components most affected by diffusion are first poorly represented in, and then removed from, the measurement and analysis. Given a distribution of T_2 values, this results in overestimation of the average T_2 of the remaining components and an overall under estimation of the total signal amplitude. The best estimate of T_2 is made in the limit $\tau = 0$. However, in the subsequent discussion, data recorded with $\tau = 12$ μs have been used as a good approximation to this.

For the 97% RH tile, the three components have T_2 values of 56 μs, 296 μs and 1.75 ms with amplitudes per unit volume of tile of 0.14, 0.07 and 0.03, respectively, where the amplitudes are normalized to unit signal per unit volume of water. The normalized amplitudes give a direct measure of the hydrated porosity of the sample. The total hydrated porosity as measured by

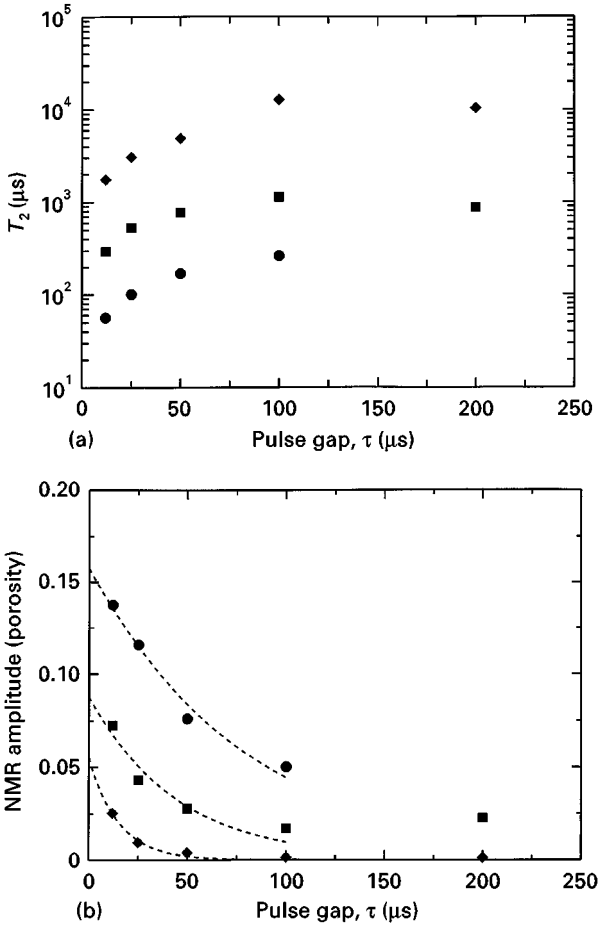

Figure 4 (a) The spin–spin relaxation time, T_2, for each of three fitted components (●, ■, ◆) for the 97% RH tile as a function of pulse gap and (b) the corresponding amplitudes.

NMR for this sample is therefore 23%, considerably more than the mercury intrusion porosimetry result would suggest is possible, but also considerably less than full saturation according to water suction data [9].

Accordingly, we have made similar CPMG measurements on an oven-dried and subsequently vacuum-saturated tile. The tile increased in mass by 16.75%, a little more than the 15.6% of the 97% RH tile and broadly consistent with the earlier result of Raoof and Sabouraud [9]. However, the CPMG decay, shown in Fig. 3c is strikingly different. Although the overall amplitude of the CPMG decay and of its separate components is consistent with the earlier data, the observed T_2 values of 159 μs (amplitude, 0.13), 1.61 ms (amplitude, 0.07) and 13.7 ms (amplitude, 0.03) are much longer. We attribute the large change in the relaxation times to changes in the pore morphology brought about by the saturation procedure.

In an attempt to account for the discrepancy between the NMR and suction data, the amplitude curves of Fig. 4b have been extrapolated back to zero pulse gap. On the basis of the broken curves in Fig. 4b, the hydrated porosity of the 97% RH tile is 29.8%. Given that this tile is only 15.6/17.2 = 91% saturated, this gives a total porosity of 33%, in excellent agreement with the suction data.

The fast diffusion model of relaxation is widely applied to water relaxation in porous media [4] and is based on the idea that the observed spin–spin relaxation rate, $1/T_2^{\text{obs}}$, of water in a given pore is the weighted average of the relaxation rate, $1/T_2^{\text{bulk}}$, of bulk water in the body of the pore and the relaxation rate, $1/T_2^{\text{surface}}$, of water in the layer in contact with the pore surface

$$\frac{1}{T_2^{\text{obs}}} = \frac{f^{\text{bulk}}}{T_2^{\text{bulk}}} + \frac{f^{\text{surface}}}{T_2^{\text{surface}}} \tag{1}$$

where f^{bulk} and f^{surface} are the fractions of water in the bulk and surface sites, respectively. For a fully saturated pore of radius, r, the fraction of water in the surface layer, of thickness, λ, is given by

$$f^{\text{surface}} = \frac{3\lambda}{r} \tag{2}$$

whilst the fraction in the bulk is given by

$$f^{\text{bulk}} = 1 - \frac{3\lambda}{r} \tag{3}$$

The surface layer thickness is generally taken as the thickness of a monolayer of water, λ = 30 nm so that for the pore sizes in question $r \gg \lambda$. Moreover, the T_2 of bulk water is of the order of a few seconds, say 1 s, whilst that of the surface layer is much shorter. Although it is strictly unknown, a good estimate can be taken from the T_2 of the hydration products of the cement with which the water is in intimate contact, say of the order of 7 μs. Consequently, for pores on the micron scale, only the second term in Equation 1 is important and the observed spin spin relaxation time is taken as

$$\frac{1}{T_2^{\text{obs}}} = \frac{3\lambda}{r}\frac{1}{T_2^{\text{surface}}} \tag{4}$$

We therefore immediately associate the three observed relaxation components in the fully saturated tile with three characteristic pore sizes, and indeed the shortest component with the smallest pore size up to the longest with the largest pore size. On this basis the pore sizes evaluate to 0.007 μm, 0.038 μm and 0.22 μm, respectively, using the relaxation times for the 97% RH tile. The relative amplitudes of the three NMR components correspond directly with the total volume in each of the three pore sizes. They are clearly unequal, with the smallest pores showing greatest volume.

Using the data for the vacuum-saturated tile gives pore sizes of 0.021 μm, 0.21 μm and 1.76 μm, in surprisingly good agreement with the mercury porosimetry results although the relative volumes differ from the mercury porosimetry, with the NMR showing greater volume in small pores, perhaps because the mercury fails to invade them. We have already suggested that damage may have occurred to the pore structure of the fully saturated sample during preparation. If this is the case, then it is possible that similar damage to the pore structure occurred in the preparation of the mercury intrusion sample also. We finally note that each NMR relaxation component is likely to represent a distribution of relaxation times and hence a distribution of pore sizes. Whilst detailed analysis of relaxation distributions has been performed for other systems [12] and has been attempted in this study

using stretched exponentials, the signal-to-noise ratio of the current data does not allow firm conclusions to be drawn in this case.

At lower hydrations, the NMR amplitudes continue to reflect water concentrations, and the T_2 values reflects the surface-to-volume ratio of the water in the pore space. For example, if it is assumed that at intermediate saturation all the pores of a given size are uniformly saturated, and that the water covers the water wet pore surfaces to a uniform depth h, then Equation 1 is evaluated to be

$$\frac{1}{T_2^{\text{obs}}} = \left(1 - \frac{3\lambda}{3h - 3h^2/r + h^3/r^2}\right)\frac{1}{T_2^{\text{bulk}}} + \left(\frac{3\lambda}{3h - 3h^2/r + h^3/r^2}\right)\frac{1}{T_2^{\text{surface}}} \quad (5)$$

which, in the intermediate regime of $\lambda \ll h \ll r$ is evaluated to be

$$\frac{1}{T_2^{\text{obs}}} = \frac{\lambda}{hT_2^{\text{surface}}} \quad (6)$$

In this case, T_2 increases with increasing saturation to a maximum value at full saturation. Such behaviour has been widely reported for porous silica glasses [13, 14] and for rocks [15]. On the other hand, if some pores fully saturate and some remain empty at intermediate hydration levels, then the T_2 value is not expected to change, although the signal amplitude will be reduced from that at full saturation.

We first look at the amplitudes of the three fitted components. These are shown in Fig. 5. From this figure, it is clear that the total amplitude of the CPMG echo train increases linearly with increasing sample hydration as might be expected. However, the individual components do not. There is a clear trend by which the shortest component, corresponding to water in the smallest pores, preferentially increases, indicating that the small pores fill first. The large pores do not fill appreciably at hydrations corresponding to less than 11% mass uptake. The total amplitude data can be extrapolated back to intercept the amplitude axis at about 0.04. This indicates a residual hydrated porosity in the so-called dry tile of about 4% corresponding to water which is not seen by either gravimetric or mercury porosimetry.

The relaxation time constants themselves are shown in Fig. 6 as a function of hydration. It is immediately

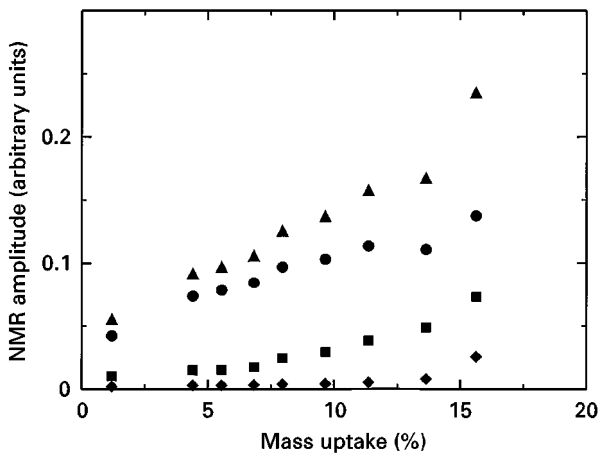

Figure 5 The amplitudes of the short (●), intermediate (■) and long (◆) T_2 components for the series A-UP tile as a function of water content together with the total amplitude (▲).

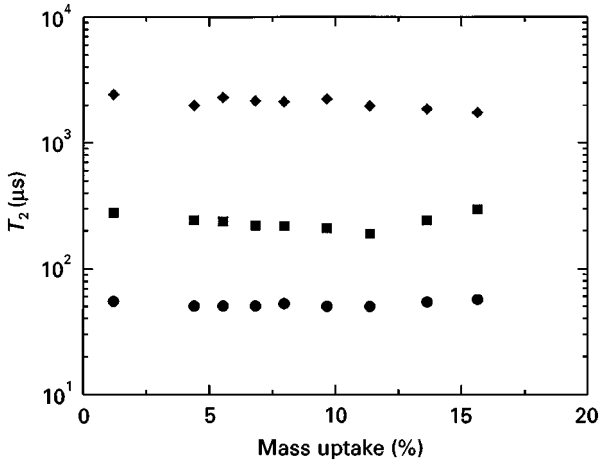

Figure 6 The T_2 values of the short (●), intermediate (■) and long (◆) T_2 components for the series A-UP tile as a function of water content.

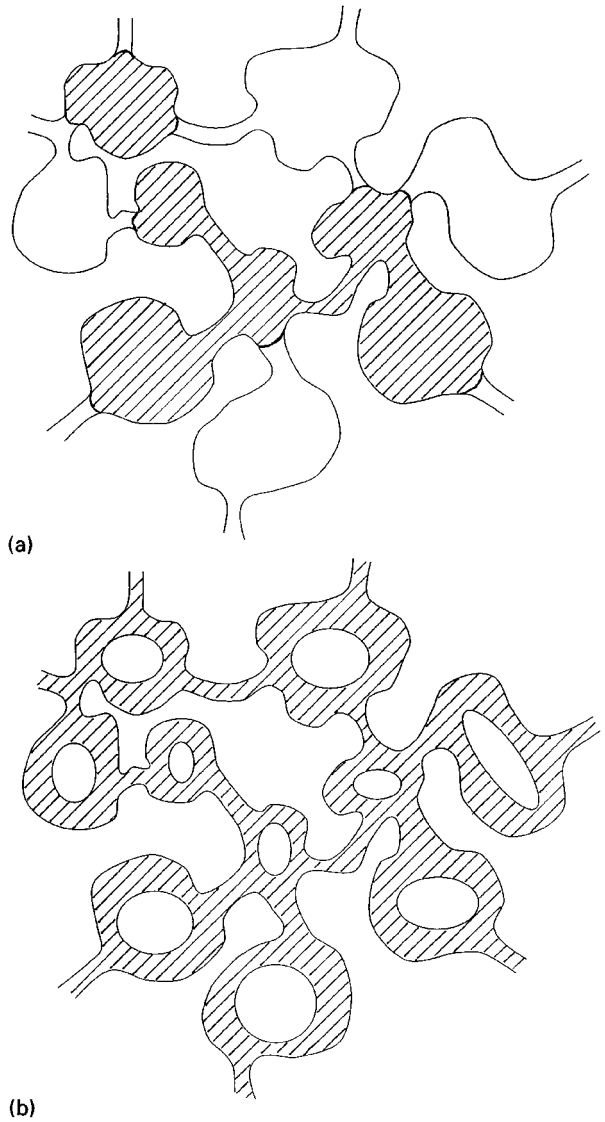

Figure 7 (a) A schematic diagram of the water distribution inside the tile pore space at intermediate hydrations as suggested by the NMR analysis. (b) An alternative distribution for partially filled pores as described by Equation 5.

evident that, unlike porous silica glasses and many rocks, the T_2 of each component remains remarkably constant over the full hydration range. This strongly suggests that, within each pore size grouping, some pores are completely filling whilst others are remaining empty. This situation is represented by Fig. 7a. The alternate scenario of partially filled pores as described by Equation 5 and as found in the glasses and rocks is shown for comparison in Fig. 7b. We suggest that this result is explained in the tiles by a small quantity of hydrophobic additive within the filler in the manufacturing mix which makes the pore surfaces hydrophobic, thus causing the water to aggregate.

3.2. Spatially resolved measurements

Fig. 8 shows the profiles of each of four tile samples (series A-UP & B-UP, outer or inner surface exposed to water), after drying but before the addition of water, after 30 h exposure to water and again after 95 and 195 h. In each case the first profile is a composite of the dry tile and the epoxy used to seal the tile in the tube. This signal forms a baseline offset for the water ingress profiles which are shown again in Fig. 9 but with the dry profile subtracted. The signal from the bulk water above the tiles is seen rising to the right of the profiles. From these profiles it is immediately clear that the bulk of the water is taken up during the first 30 h. The similarity between the profiles recorded after 30, 95 and 195 h suggests that the water distribution in the tile has, in each case, attained a dynamic equilibrium in which the supply of water on one side is matched by evaporative losses on the other. It is noticeable that in the series A-UP samples the water profile shows strong heterogeneity in terms of three layers, which it is logical to assume correspond to the three layers of the tile. The low intensity at each of the layer interfaces probably corresponds to a reduced porosity brought about by the three successive cycles of compression during tile manufacture. We note that the water concentration is greatest within the external layer of the tile, irrespective of whether the water enters from the inner or outer surface. A reverse concentration gradient in a transport experiment, as observed in Fig. 9b, can only be achieved if the available porosity is not uniform across the tile. We therefore propose that at low water concentrations the external layer of the tiles has a significantly greater pore volume available to water than the inner surface layer. If, as believed, the external layer corresponds to the region of smallest pores, then such a conclusion is consistent with the bulk T_2 analysis already described. One plausible explanation of the diffusion is that the water transport mechanism involves rapid vapour transport through the connected pore structure coupled with much slower capillary transport of

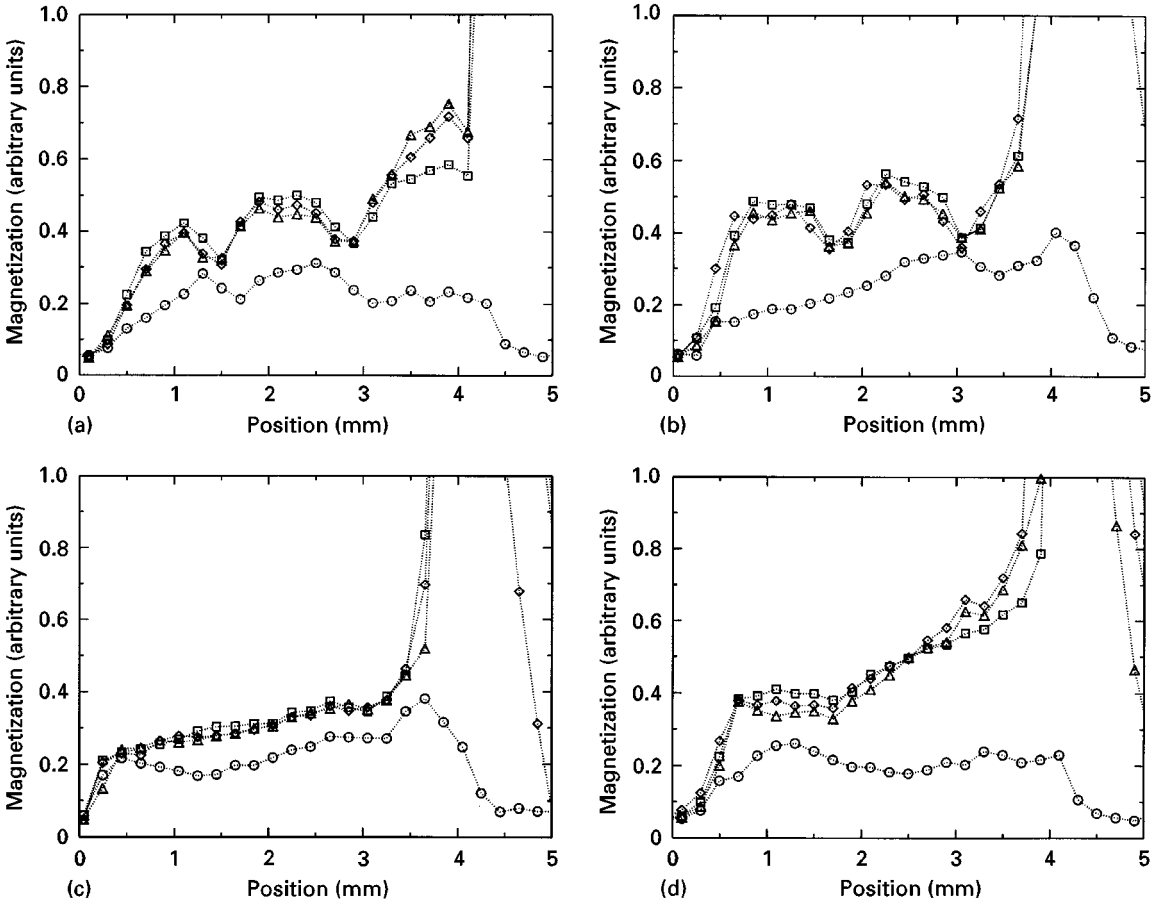

Figure 8 The as-recorded profiles of water content in (a) an untreated (A-UP series) tile with the outer surface exposed, (b) an untreated tile with the inner surface exposed, (c) a treated (B-UP series) tile with the treated outer surface exposed and (d) a treated tile with the inner, untreated surface exposed to water after 0 h (○), 30 h (□), 95 h (◇) and 195 h (△). In every case, the 0 h profile is a composite of the dry tile and the epoxy resin used in the sample preparation. In subsequent profiles, the bulk water is seen as the peak to the right.

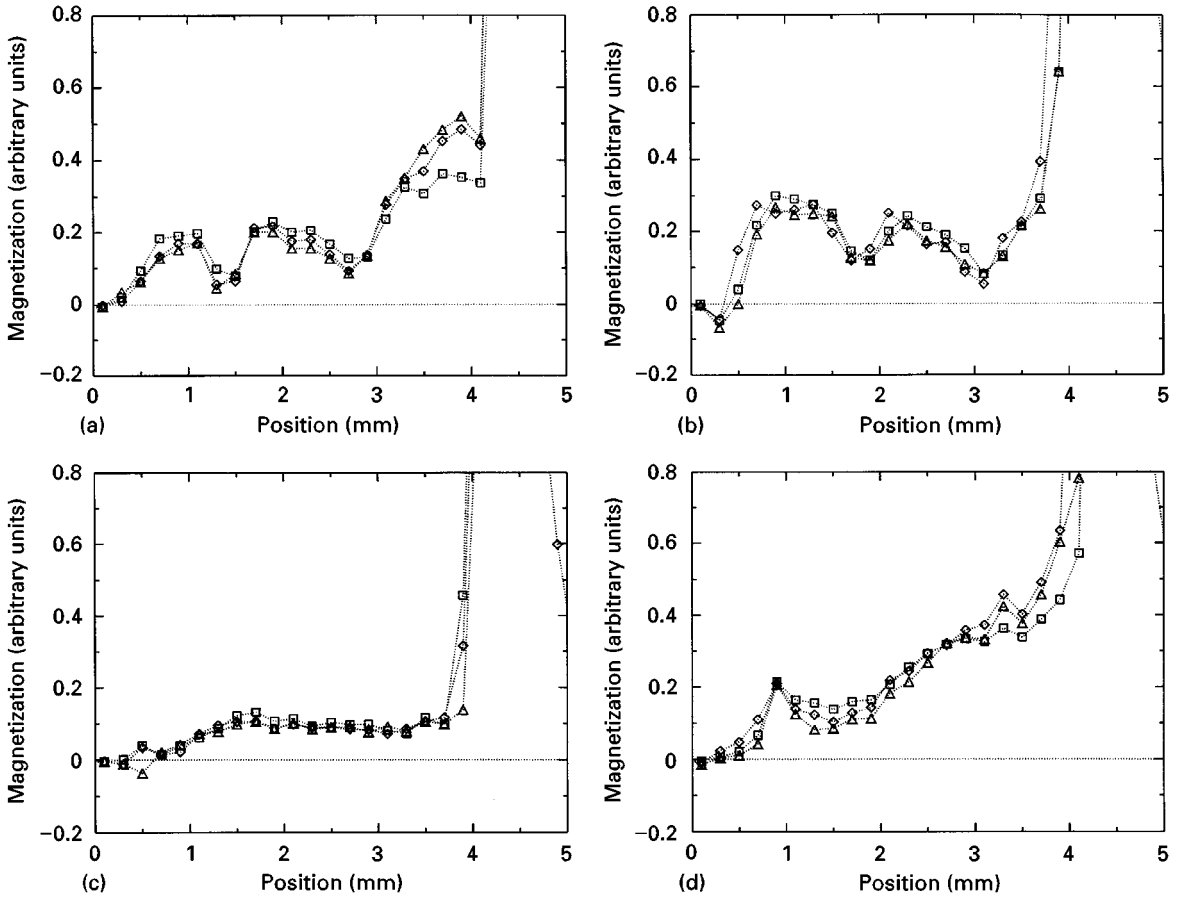

Figure 9 As Fig. 8, except that the dry profile has been subtracted.

liquid. Certainly, nothing in the observed data is contrary to this suggestion. However, given the large-scale structural heterogeneity of the tiles, it is difficult to make a more quantitative analysis as has been achieved with, for instance, water transport in porous zeolite powder beds [16] and sandstone rocks [17].

In the case of the surface-treated tile, series B-UP, the structural heterogeneity is much less evident. As might be expected, there is considerably less water in the tile with the treated surface exposed. This is due to a much lower water transport rate through the treated layer than through rest of the tile and the consequent effect that this has on the profile via the detailed balance of water supply and water loss. When the treated layer is exposed to water, the slow ingress of water through the treatment layer and relatively rapid drying from the untreated side together maintain a very low water concentration profile throughout the bulk of the tile. On the other hand, when the inner surface is exposed to water rapid ingress and slow egress now ensure a much higher concentration level in the bulk of the tile as observed.

Fig. 10 shows profiles, with the dry profile subtracted, acquired over the first 30 h of a second water uptake experiment. These profiles are acquired at 38 min intervals. In Fig. 10a the external surface of an untreated tile is exposed to water and in Fig. 10b the external surface of a treated tile. Fig. 11 is a plot of the water front position measured at half the surface concentration as a function of time. The solid curve in the plot is a fit to the function $x = At^{1/2}$ (A constant), which strongly suggests that the water transport is determined by generalized Fickian diffusion governed by

$$\frac{\partial c}{\partial t} = \frac{\partial}{\partial x}\left(D(c)\frac{\partial c}{\partial x}\right) \tag{7}$$

where c is the water concentration in the tile, $D(c)$ is the concentration-dependent diffusion coefficient of the water in the tile, and x and t are position and time, respectively. The structural heterogeneity of the tile makes it difficult to apply the Boltzmann transformation to these data from which the concentration dependence of the water transport diffusion constant could be deduced, as is commonly done with NMR profile data of this sort [18]. Consequently a much more simplistic data analysis has been performed which assumes a constant diffusion coefficient for the water ingressing a homogeneous material. On this basis the concentration profiles assume the form [19]

$$c(x) = c_0 \operatorname{erfc}\left(\frac{x}{2(Dt)^{1/2}}\right) \tag{8}$$

where c_0 is the surface concentration. Using the best fit to the data presented in Fig. 11, the average diffusion coefficient evaluates to $4.0 \times 10^{-7}\,\mathrm{cm^2\,s^{-1}}$, which compares favourably with the transport diffusion coefficient of water in a number of small-pore-size porous media.

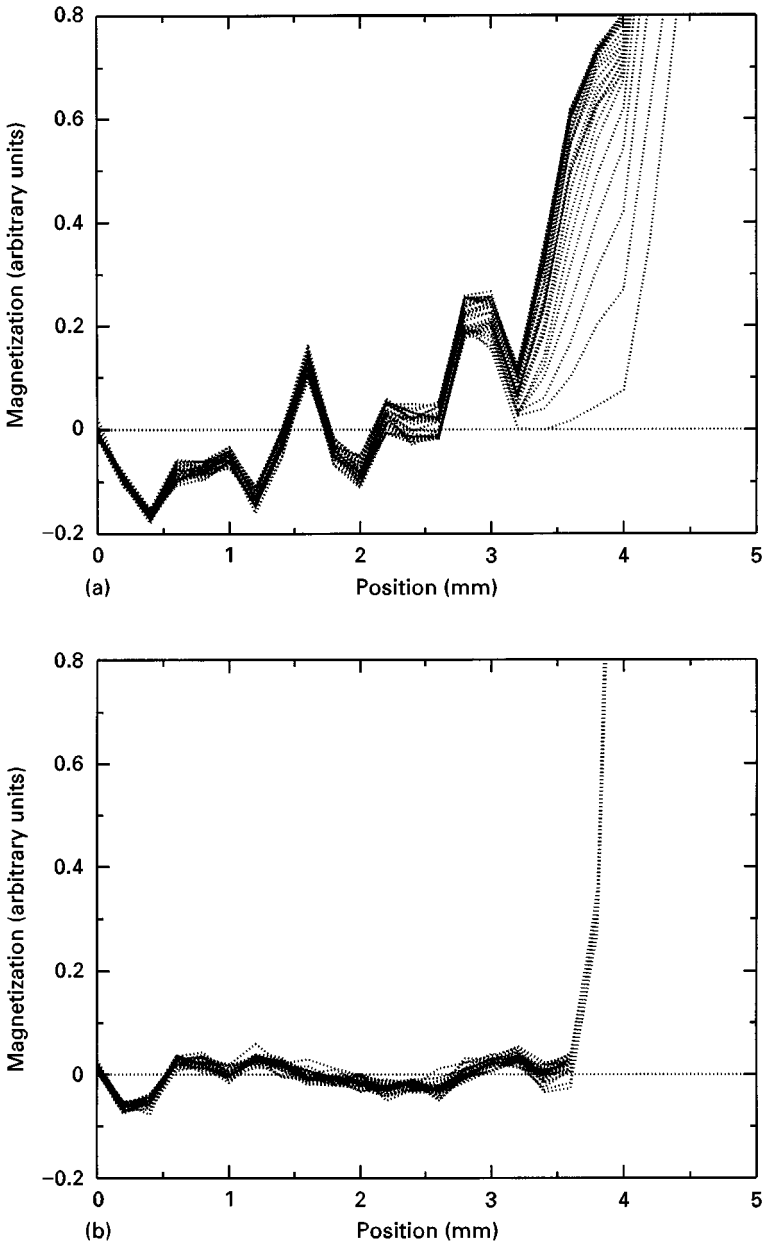

Figure 10 Profiles, with the dry profile subtracted, of (a) an untreated and (b) a treated slate, each with the outer surface exposed to water, recorded at 38 min intervals after exposure.

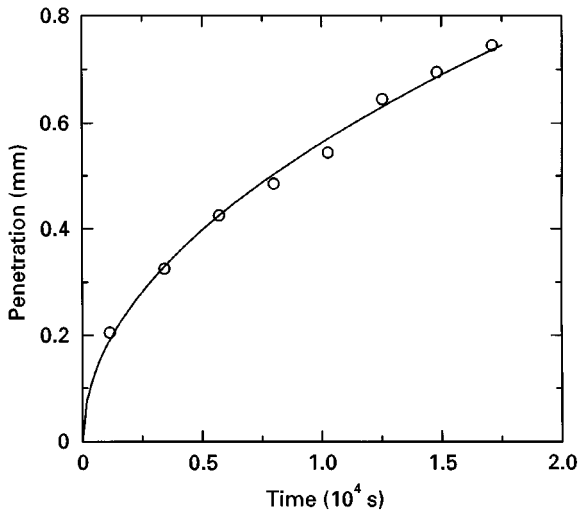

Figure 11 The water front position measured at half the surface concentration level taken from the data in Fig. 10a as a function of time and (——), fit to the function $x = At^{1/2}$.

4. Conclusion

We have shown that a combination of broad-line, bulk and spatially resolved NMR measurements are able to yield a considerable amount of information on water absorption and transport in roofing tile material. We have obtained evidence for the manner in which pores fill, measured the total porosity and the average pore sizes and found evidence of residual water content in dried material and for structural heterogeneity in the tiles. We note that all the non-spatially resolved information was obtained using bench-top NMR apparatus of the kind widely found in food and other manufacturing industry research laboratories, although less widely in laboratories associated with the building industry. Finally we note that this kind of analysis is not restricted to just roofing tiles, but can be applied more widely to other cementitous products.

Acknowledgements

The authors thank Dr M. Mulheron for many useful discussions, the UK Engineering and Physical Sciences Research Council for a research grant and the British Council and French Ministry for Foreign Affairs for financial support through the Alliance programme.

References

1. M. E. SMITH and J. H. STRANGE, *Measurement Sci. Technol.* **7** (1996) 449.
2. R. KIMMICH, "NMR, tomography, diffusion and relaxometry" (Springer, Berlin, 1997).
3. G. GUILLOT, L. DARASSE, A. TROKINER and A. DUPAS, *Pour la Science* **154** (1990) 16.
4. W. P. HALPERIN, J.-Y. JEHNG and Y.-Q. SONG, *Magn. Reson. Imaging* **12** (1994) 169.
5. J.-Y. JEHNG, D. T. SPRAGUE and W. P. HALPERIN, *ibid.* **14** (1996) 785.
6. E. LAGANAS, G. PAPAVASSILIOU, M. FARDIS, A. LEVENTIS, F. MILIA, E. CHANIOTAKIS and C. MELETIOU, *J. Appl. Phys.* **77** (1995) 3343.
7. A. A. SAMOILENKO, D.-Yu. ARTEMOV and L. A. SIBEL'DINA, *JETP Lett.* **47** (1988) 147.
8. P. J. McDONALD, *Prog. NMR Spectrosc.* **30** (1997) 69.
9. A. RAOOF and A. SABOURAUD, *Mater. Struct.* (1997) (in press).
10. R. A. COOK, K. C. HOVER and O. Z. CEBECI, *ACI Mater. J.* **91** (1994) 119.
11. S. MEIBOOM and D. GILL, *Rev. Sci. Instrum.* **29** (1956) 688.
12. P. P. MITRA and P. N. SEN, *Phys. Rev. B* **45** (1992) 143.
13. F. D'ORAZIO, S. BHATTACHARJA, W. P. HALPERIN, K. EGUCHI and T. MIZUKAKI, *ibid.* **42** (1990) 9810.
14. A. RAOOF, PhD thesis, University of Marne la Vallée, Chap. 4, (1997).
15. S. P. ROBERTS, P. J. McDONALD and T. PRITCHARD, *J. Magn. Reson. A* **116** (1995) 189.
16. P. D. M. HUGHES, P. J. McDONALD and E. G. SMITH, *ibid.* A **121** (1996) 147.
17. P. J. McDONALD, T. PRITCHARD and S. P. ROBERTS, *J. Colloid Interface Sci.* **177** (1996) 439.
18. P. MANSFIELD, R. BOWTELL and S. BLACKBAND, *J. Magn. Reson.* **99** (1992) 507.
19. J. CRANK, "The mathematics of diffusion" (Oxford University Press, Oxford, 1975).

Received 9 May
and accepted 24 September 1997